Jurnal E-Komtek
Vol. 9, No. 2. (2025) pp. 709-723
https://jurnal.politeknik-kebumen.ac.id/index.php/E-KOMTEK
p-ISSN : 2580-3719 e-ISSN : 2622-3066

Modeling and Optimization of PET Filament Making Machine Control System Based on Response Surface Methodology

Deni Nur Fauzi[1], Pradhana Kurniawan[1], Imam Junaedi[2], Rendi Pambudi Wicaksono[3], Nabila Bilqis Mahardi[2]

[1] Department of Automotive Engineering Technology, Politeknik Negeri Madiun, Indonesia, 6316
[2] Department of Computer Control, Politeknik Negeri Madiun, Indonesia, 6316
[3] Department of Electronic Engineering Technology, Politeknik Negeri Madiun, Indonesia, 6316

deninurfauzi@pnm.ac.id

https://doi.org/10.37339/e-komtek.v9i2.3017

Published by Politeknik Piksi Ganesha Indonesia

Artikel Info
Submitted:
28-01-2026
Revised:
29-01-2026
Accepted:
29-01-2026
Online first :
29-01-2026

Abstract

This study aims to model and optimize the control system of a PET filament making machine using Response Surface Methodology (RSM). Two main variables, namely extrusion temperature and winding speed, were analyzed through the Central Composite Design experimental design with the help of Design-Expert 13 software. A quadratic model was developed to predict the filament diameter, and the results of the analysis of variance showed that the model was statistically significant and able to represent the nonlinear relationship between variables. Optimization based on the desirability function produced optimum operating conditions at a medium temperature and winding speed range. Experiments showed that the combination of a temperature of 240–245 °C and a speed of 9–12 rpm produced a consistent filament diameter of 1.7 mm with 70–80% flexibility and a smooth surface.

Keywords: *PET filament making machine; Control system; Response Surface Methodology (RSM); Process parameter optimization; Recycled filament.*

Abstrak

Penelitian ini bertujuan memodelkan dan mengoptimasi sistem kendali mesin pembuat filamen PET menggunakan Response Surface Methodology (RSM). Dua variabel utama, yaitu suhu ekstrusi dan kecepatan penggulungan, dianalisis melalui desain eksperimen Central Composite Design dengan bantuan perangkat lunak Design-Expert 13. Model kuadratik dikembangkan untuk memprediksi diameter filamen, dan hasil analisis varians menunjukkan model signifikan secara statistik serta mampu merepresentasikan hubungan nonlinier antar variabel. Optimasi berbasis fungsi desirability menghasilkan kondisi operasi optimum pada rentang suhu dan kecepatan penggulungan menengah. Eksperimen menunjukkan bahwa kombinasi suhu 240–245 °C dan kecepatan 9–12 rpm menghasilkan filamen berdiameter konsisten 1,7 mm dengan kelenturan 70–80% dan permukaan halus.

***Kata-kata kunci**: Mesin pembuat filamen PET; Sistem kendali; Response Surface Methodology (RSM); Optimasi parameter proses; Filamen daur ulang.*

1. Introduction

The development of 3D printing technology has experienced rapid growth in recent years. One key aspect of this technology's success is the availability of filament materials that have stable quality, good mechanical properties, and can be produced efficiently and environmentally friendly. Polymers based on polyethylene terephthalate (PET) and its derivatives, such as PETG, have been widely used in 3D printing applications due to their combination of superior thermal and mechanical properties, and ease of processing compared to other thermoplastic polymers **[1], [2].**

Various studies have shown that recycled PET (rPET) has great potential as a 3D printing filament material, both in terms of mechanical strength and environmental sustainability **[3], [4], [5]**. The use of rPET in 3D printing not only reduces reliance on virgin polymers but also directly contributes to the reduction of plastic waste. However, PET filament making machines must be able to precisely control the heating, extrusion, cooling, and winding stages to ensure the resulting filament has a uniform diameter and consistent mechanical properties. Previous research has shown that the flow characteristics of PET melts are strongly influenced by processing temperature and material composition, where small changes in temperature can significantly impact viscosity and flow stability **[3].**

In addition to temperature, the tensile force generated by the winding system also plays a critical role in determining filament diameter and quality. The relationship between extrusion rate and winding speed is interconnected and often exhibits nonlinear behavior. Studies related to rPET printing have shown that although filaments can be produced from plastic bottle waste with reasonably good mechanical properties, the final quality of the printed product is highly dependent on the filament's dimensional stability during the printing process **[4]**. Therefore, PET filament making machines require a control system capable of simultaneously maintaining a balance between extrusion temperature and winding speed.

Processing temperature has a dominant influence on the viscosity of polymer melts. In PET-based materials and their derivatives, small changes in temperature can cause significant changes in the melt flow rate (MFR) or melt flow index (MFI). Previous research has shown that materials with lower melt flow rates tend to produce more uniform print layers, thereby improving surface quality and dimensional consistency of the print **[6].** This confirms that

controlling the extrusion temperature is not only aimed at melting the material but also at regulating optimal flow characteristics for the filament formation process.

In addition to temperature, the filament winding speed plays a role in controlling the tensile force. Experimental studies on the production of recycled PET filaments have shown that stable filament diameter can only be achieved when the heating and winding systems are precisely and repeatably controlled **[7].** Several studies focusing on PET and PETG-based filaments, including composite filaments and blended filaments, have shown that imbalanced process parameters can lead to decreased mechanical properties due to the formation of porosity, uneven shrinkage, and microstructural irregularities **[8], [9].**

Studies have shown that the mechanical properties of printed products, such as ultimate tensile strength and Young's modulus, are highly sensitive to filament consistency and subsequent printing parameters such as layer height and infill density **[10].** Therefore, temperature and winding speed control systems on PET filament making machines are necessary to ensure that the resulting filaments have close to the target diameter, a smooth surface, and reproducible mechanical properties. However, the complex and nonlinear characteristics of the PET filament extrusion process make determining optimal control parameters a challenge. Trial-and-error approaches are often inefficient and difficult to reproduce, especially when there are interactions between process parameters. Therefore, a systematic modeling and optimization approach is needed to analyze the effects of temperature and winding speed simultaneously. In this context, statistical modeling methods such as Response Surface Methodology become relevant for use as a tool for analyzing and optimizing PET filament machine control systems. Therefore, a statistical method is needed that can build predictive models while supporting the parameter optimization process in a systematic and structured manner **[11].**

Response Surface Methodology (RSM) has been widely used as an integrated framework for modeling and optimizing process parameters in various engineering and applied science fields. RSM combines experimental design, statistical analysis, and mathematical modeling to evaluate linear, quadratic, and interaction effects between process variables. The advantages of this method have been demonstrated in various applications, such as chemical analysis process optimization, materials engineering, and manufacturing systems, where RSM models are able to provide predictions that closely match actual experimental results with a high degree of accuracy **[11], [12], [13].**

In the modeling stage, RSM generally uses experimental designs such as Central Composite Design (CCD) or Box–Behnken Design (BBD) to build second-order mathematical models. This approach allows for the evaluation of the significance of process parameters and their interactions through analysis of variance (ANOVA), thus identifying the most important factors. The factors influencing system response can be identified objectively. The application of CCD and BBD has proven effective in modeling complex processes, both in multistage thermodynamic systems and precision machining processes with high tolerances **[12], [14], [15]**.

Besides being a modeling tool, RSM is also used in process parameter optimization using the desirability function approach. Various studies have shown that RSM-based optimization can produce optimal and technically realistic operating conditions, with predicted results validated through actual experiments, both in multistage cooling systems, high-pressure extraction processes, and engineering systems **[12], [14].**

RSM presents analysis results in visualizations that facilitate interpretation of the relationships between process parameters and the identification of the optimum operating region, which is often more practically relevant than a single optimum point **[16], [17], [18].** This optimum region-based approach has been effectively applied in energy systems, environmental processes, and precision manufacturing to determine safe and efficient parameter ranges **[11], [14]**. RSM is also capable of uncovering parameter interactions that were previously difficult to explain experimentally and provides a scientific basis for improving process quality [11], [14], **[19]**.

Based on this review, the application of Response Surface Methodology-based modeling and optimization is highly relevant for PET filament machine control systems. This system involves extrusion temperature and winding speed, which interact and directly influence the filament diameter response. Using RSM, the relationship between control system parameters and filament quality can be quantitatively modeled, and the optimal operating region can be systematically determined and validated through actual experimental results. This approach provides a solid scientific foundation for developing stable, efficient, and reliable PET filament machine control systems for 3D printing applications.

2. Method

This section will explain the system block diagram, the operating principle of the device, a flowchart of the road damage detection and dimension estimation system, and techniques for data analysis.

2.1 System Block Diagram

This section will explain the system block diagram (Figure 1), the operating principle of the device, the flowchart for the road damage detection and dimension estimation system, and the data analysis techniques.

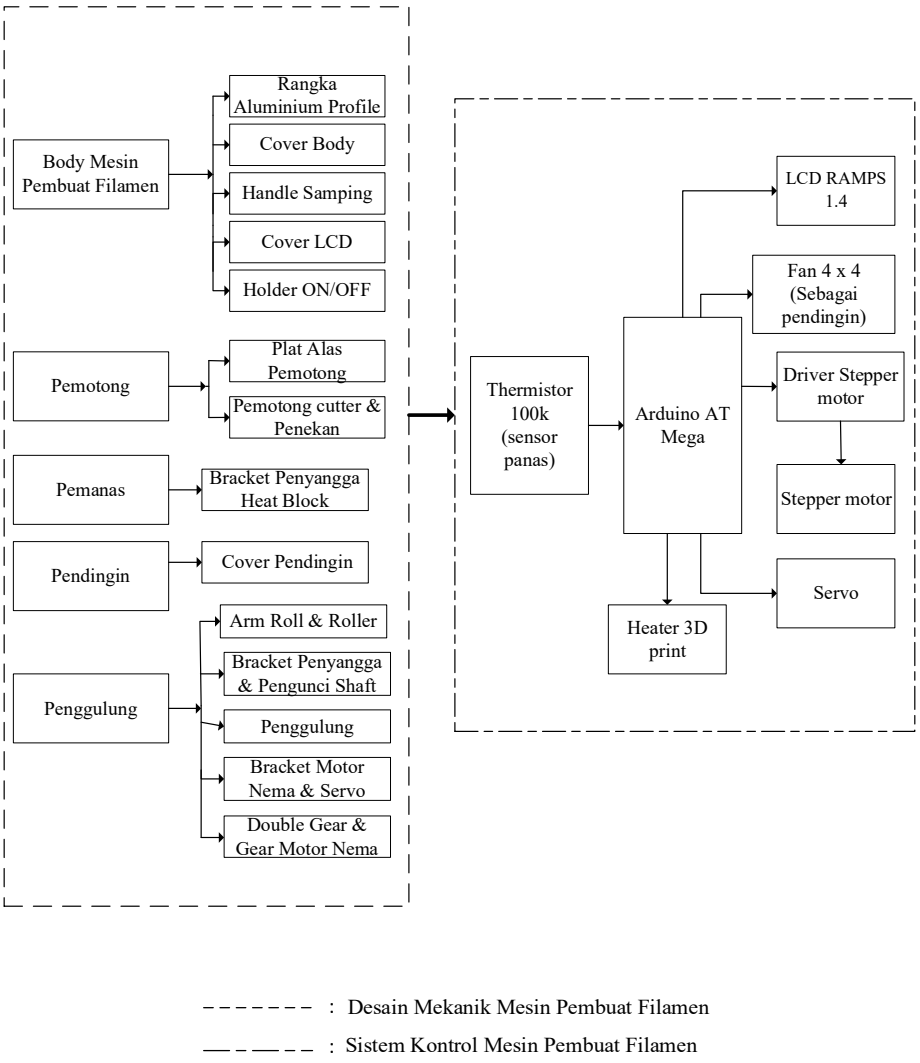

Figure 1. Block Diagram

Figure 2 shows that this filament making machine has a control system that uses an Arduino ATmega as its microcontroller, a 100k thermistor as a heat sensor, and uses several actuators, namely LCD Ramps, a 2.5 cm x 2.5 cm fan, a driver and stepper motor, a servo, and a 3D print heater.

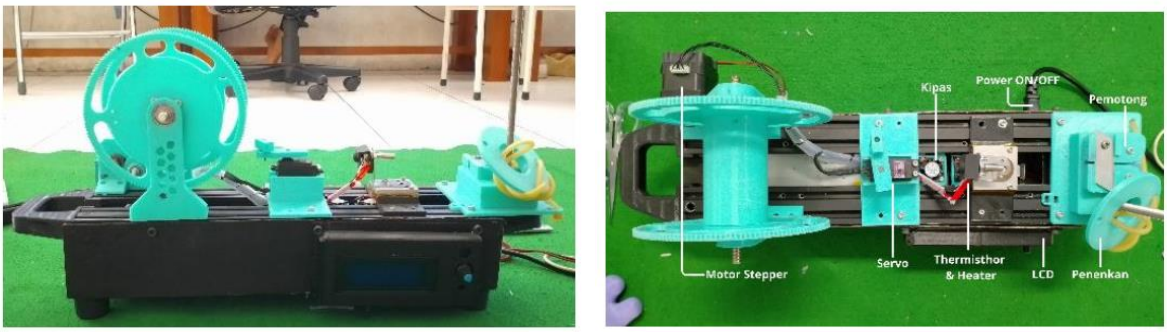

Figure 2. Filament Machine with Arduino ATmega

2.2 Working Principle of the Tool

Figure 3 shows the working principle of the control system tool on a 3D print filament making machine using used PET bottles as the base material.

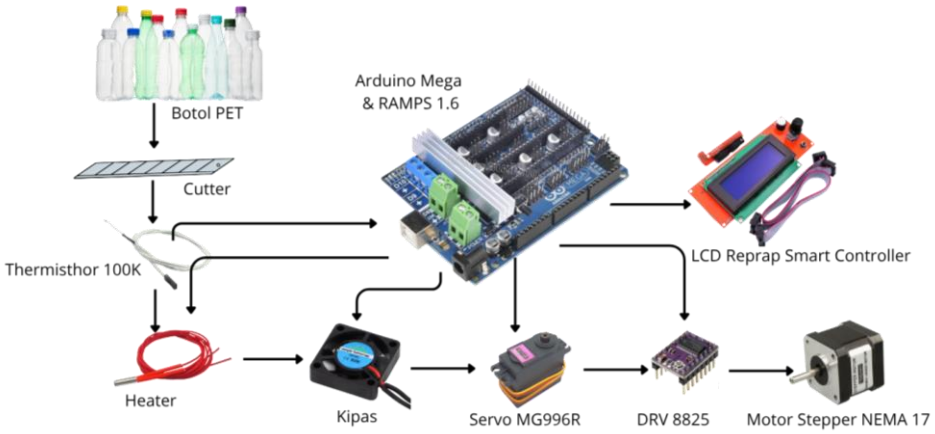

Figure 3. Working Principle of the Tool

This system uses an Arduino Mega microcontroller to control the PET bottle recycling process into 3D printing filament. The process begins with heating the PET bottle to flatten its shape, then the tip of the bottle is cut to a point. The cut tip of the bottle is then further processed with a cutter to produce a 7mm wide cut. After that, the PET bottle is melted using a heater, with temperature settings controlled by a 100k thermistor and formed using a nozzle. Then cooled by a fan, then the filament is rolled by a stepper motor with the help of a servo to smooth the roll. All system status and temperature information are displayed on the RAMPS LCD, ensuring that each stage of the process runs synchronously and efficiently. The resulting 3D printing filament is approximately 1.75 mm in diameter. The 1.75 mm filament was chosen for its several advantages, such as improved extrusion, more precise material flow control for high-quality prints, and the size of the majority of 3D printers on the market.

3. Results and Discussion

This chapter will explain the results and discuss the control system for a filament-making machine using used PET bottles. This study, which has gone through several stages, from design to testing, data collection, and analysis of the results, will be presented.

3.1. Response Surface Methodology Simulation

In this study, PET filament diameter optimization was performed using Response Surface Methodology (RSM) with two main process variables: extrusion temperature (A) and winding speed (B). These two variables were chosen because they directly affect the stability of the polymer melt flow and the consistency of the filament diameter.

Table 1. 3D Printing Experiment Results

Run	Factor 1	Factor 2	Response 1
	A:Extrusion Temperature	B: Roller Speed	Filament Diameter
	°C	rpm	mm
1	245	12	1.7
2	245	12	1.71
3	245	12	1.69
4	240	12	1.68
5	245	15	1.65
6	250	9	1.67
7	245	9	1.69
8	240	15	1.64
9	250	15	1.63
10	245	12	1.7
11	245	12	1.71
12	240	9	1.66
13	250	12	1.66

Based on the Table 1 used, the extrusion temperature varied within the range of 240–250 °C, while the winding speed varied within the range of 9–15 rpm. Each variable was coded into three levels (−1, 0, +1) to allow for analysis of linear, quadratic, and interaction effects between

the variables. This coding approach is commonly used in RSM because it normalizes the scale of variables and improves the stability of statistical models [20].

The experimental design matrix consisted of 13 experimental runs, including a repeated center point to estimate pure error. Each run represented a unique combination of extrusion temperature and winding speed, with the response being filament diameter (mm). The use of this relatively small but informative number of runs is an advantage of RSM-based DOE over single-variable-at-a-time methods, as it captures interaction effects and nonlinearities more efficiently with less experimental cost [21], [22].

Table 2. Lack of Fit Tests

Source	Sum of Squares	df	Mean Square	F-value	p-value	
Linear	0.0065	6	0.0011	15.46	0.0097	
2FI	0.0064	5	0.0013	18.27	0.0074	
Quadratic	**0.0003**	**3**	**0.0001**	**1.27**	**0.3984**	**Suggested**
Cubic	0.0001	1	0.0001	1.42	0.2995	Aliased
Pure Error	0.0003	4	0.0001			

The lack of fit test (**Table 2**) was used to evaluate the suitability of the statistical model to the experimental data. For the selected quadratic model, the p-value for lack of fit was 0.3984, which is greater than 0.05. This indicates that the lack of fit is insignificant, indicating that the model adequately represents the experimental data. An insignificant lack of fit is a key indicator that the RSM model can be used for reliable process prediction and optimization [23], [24]. The ANOVA results for the quadratic model (**Table 3**) showed statistical significance with an F-value of 20.42 and a p-value of 0.0005. This indicates that the variation in the filament diameter response is significantly influenced by the studied process variables.

Partially, the winding speed factor (B) and the quadratic components A^2 and B^2 had p-values <0.05, indicating a significant effect on filament diameter (**Table 4**). Conversely, the linear interaction AB was not significant, indicating that the combined effect of the two variables is predominantly nonlinear. This pattern is consistent with the characteristics of manufacturing processes involving melted polymer flow [25], [26]. In the developed RSM model, Y represents the PET filament diameter (mm). This response was chosen because filament diameter is a key quality parameter in FDM applications, where even small deviations can impact 3D printing performance.

Table 3. ANOVA for Quadratic model

Source	Sum of Squares	df	Mean Square	F-value	p-value	
Model	0.0080	5	0.0016	20.42	0.0005	significant
A- Extrusion Temperature	0.0001	1	0.0001	0.8547	0.3860	
B- Roller Speed	0.0017	1	0.0017	21.37	0.0024	
AB	0.0001	1	0.0001	1.28	0.2948	
A^2	0.0019	1	0.0019	24.32	0.0017	
B^2	0.0019	1	0.0019	24.32	0.0017	
Residual	0.0005	7	0.0001			
Lack of Fit	0.0003	3	0.0001	1.27	0.3984	not significant
Pure Error	0.0003	4	0.0001			
Cor Total	0.0085	12				

Table 4. Final Equation in Terms of Coded Factors

Filamen Diameter =	
+1.70	
-0.0033	A
-0.0167	B
-0.0050	AB
-0.0262	A^2
-0.0262	B^2

This single response definition is commonly used in RSM-based manufacturing process optimization studies to achieve product dimensional stability **[27], [28].** Model fit statistics show an R^2 value of 0.9358, an Adjusted R^2 of 0.8900, and a Predicted R^2 of 0.6729 (**Table 5**). A high R^2 value indicates that more than 93% of the variation in filament diameter can be explained by the model. The Adequate Precision value = 12.9026 (>4) indicates an adequate signal-to-noise ratio, making the model suitable for design space navigation. Although there is a difference between Adjusted R^2 and Predicted R^2, this condition is still acceptable in small-scale experimental studies and is often found in polymer-based processes **[20], [29].**

Table 5. Fit Statistics

Std. Dev.	0.0088	**R^2**	0.9358
Mean	1.68	**Adjusted R^2**	0.8900
C.V. %	0.5269	**Predicted R^2**	0.6729
		Adeq Precision	12.9026

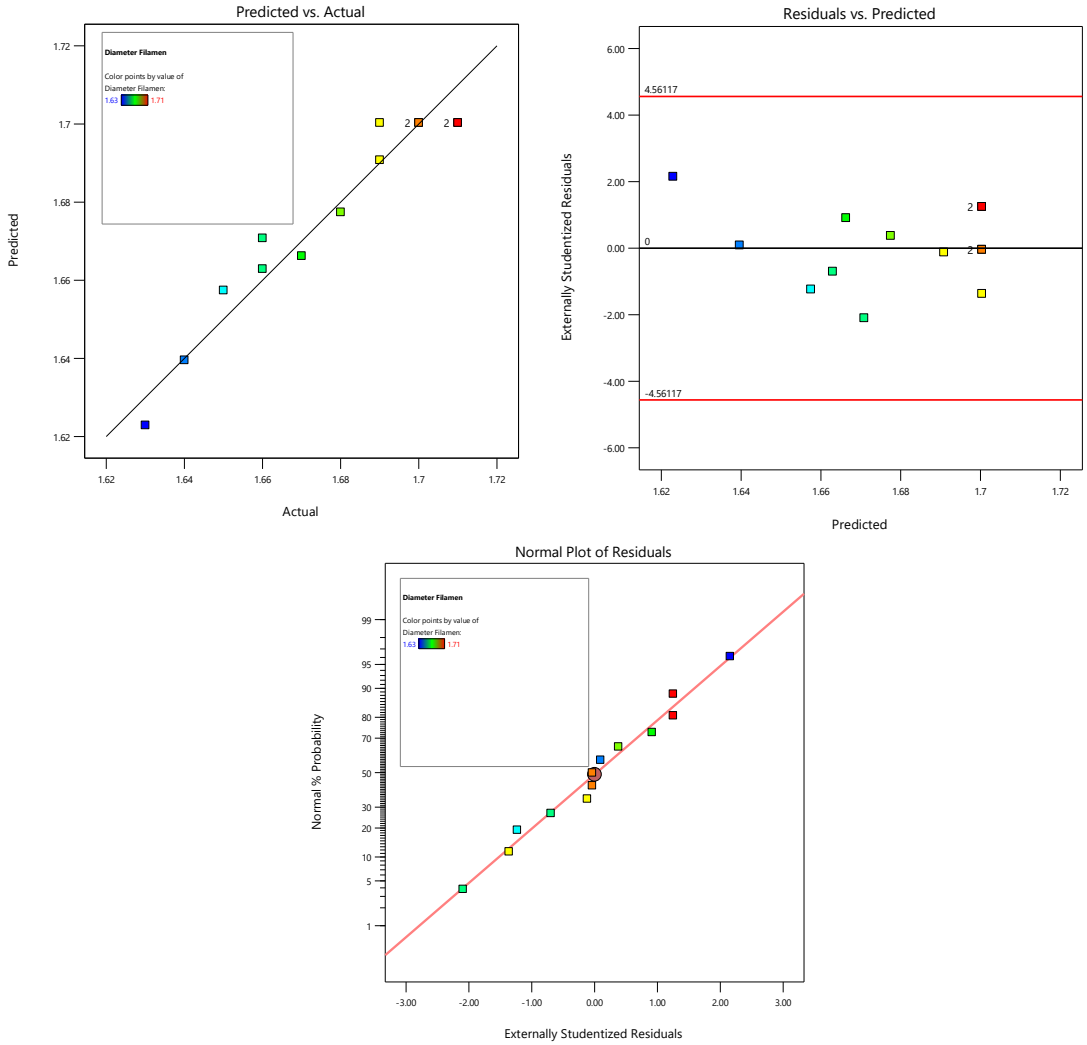

Figure 4. a) Predicted vs Actual b) Residuals vs Predicted c) Normal Plot of Reiduals

Predicted vs. Actual shows (**Figure 4a**) data points approaching a diagonal line, indicating the model's predictions match the experimental data. Residuals vs. Predicted (**Figure 4b**) show no particular pattern, thus meeting the assumption of homogeneity of variance. A normal plot of residuals (**Figure 4c**) shows a residual distribution approaching a straight line, indicating a normal distribution.

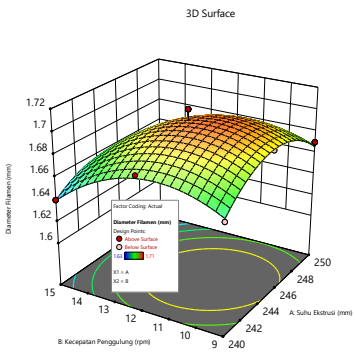

Figure 5. 3D Plot Surface

The 3D response surface plot (Figure 5) shows surface curvature, confirming the presence of a quadratic effect. The maximum filament diameter is achieved at intermediate extrusion temperatures and moderate winding speeds. This phenomenon reflects the balance between material flow rate and drawing speed, where extreme conditions in either variable tend to increase diameter fluctuations. Similar patterns have been reported in various manufacturing process optimization studies using RSM [21], [23].

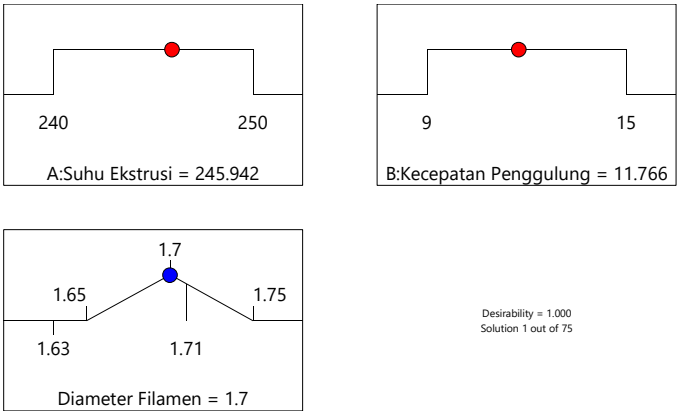

Figure 6. Plot ramp desirability

The ramp desirability plot (Figure 6) shows that the optimum combination is achieved at extrusion temperature and winding speed values around the midpoint of the operating range, with a desirability value close to 1.0. This value indicates that the optimization objective, which is to obtain a filament diameter close to the target, has been optimally achieved.

The desirability approach is widely used in RSM to unify optimization objectives into a single, easily interpretable numerical function **[20], [24].**

Based on modeling and optimization results using Response Surface Methodology (RSM), the filament diameter response exhibits nonlinear behavior with variations in extrusion temperature and winding speed. ANOVA analysis and response surface plots indicate that a significant contribution to filament diameter comes from the quadratic component of both variables, particularly in the mid- to high-range range of the tested design space. Furthermore, the optimum region identified through the ramp desirability plot lies around the midpoint of the range of winding speeds and extrusion temperatures, which are relatively operationally stable.

Based on these considerations, and to ensure repeatability and practical feasibility of the experiment, winding speed levels of 9, 12, and 15 rpm were selected to represent low, medium, and high conditions within the optimum range of the RSM simulation results. These levels were

also selected considering the sensitivity of the response shown in the perturbation plot, where winding speed exerts a more dominant influence on filament diameter variation.

Furthermore, extrusion temperatures of 240°C and 245°C were chosen as further experimental variables because they fall within the optimum range indicated by the response surface and desirability contour, and provide predicted filament diameters close to the target value with minimal variation. The selection of these two temperature levels aimed to evaluate the stability of the filament diameter response under the most technically relevant operating conditions, without expanding the temperature range to extremes that could potentially cause material degradation or process instability.

Thus, the variable combination of 9–12–15 rpm and 240–245 °C was chosen as the next experimental condition because it is statistically within the optimum region of the RSM simulation results, and practically fits the operational limits of the system. This approach is in line with RSM-based process optimization practices that recommend selecting the experimental level in the most stable and representative optimum region for experimental validation **[20], [24], [25].**

4. Conclusion

Surface Methodology (RSM) combined with an integrated control system can be effectively used to model, analyze, and optimize the PET filament manufacturing process from used plastic bottles. Using Design-Expert version 13 software, two key process variables—extrusion temperature and winding speed—were successfully modeled using a Central Composite Design-based experimental design, allowing for comprehensive analysis of linear, quadratic, and interaction relationships between the variables. ANOVA analysis results indicate that the developed quadratic model is statistically significant and adequately represents the system's behavior, as evidenced by a high coefficient of determination and an insignificant lack of fit. The winding speed parameter and the quadratic components of both variables were shown to have a dominant influence on filament diameter variation, indicating nonlinear characteristics in the recycled PET filament extrusion process. Numerical optimization based on the desirability function yielded optimum operating conditions at a moderate extrusion temperature range and moderate winding speed. Based on simulation results and process stability considerations, a combination of 240°C with a winding speed of 9 rpm and 245°C with a winding speed of 12 rpm

was selected as the experimental conditions for further experiments. Under these conditions, the system was able to produce filaments with a diameter approaching 1.7 mm, with minimal variation, and meeting standard filament tolerances for FDM-based 3D printing applications.

References

[1] V. Filho *et al.*, 'Reactive and non-reactive compatibilization of polyethylene terephthalate glycol/thermoplastic polyurethane (PETG/TPU) blends for 3D/4D printing applications', *React. Funct. Polym.*, vol. 215, p. 106393, Oct. 2025, doi: 10.1016/j.reactfunctpolym.2025.106393.

[2] K. Sandeep Varma, K. Lal Meena, and R. B. R. Chekuri, 'Optimizing mechanical properties of 3D-printed aramid fiber-reinforced polyethylene terephthalate glycol composite: A systematic approach using BPNN and ANOVA', *Eng. Sci. Technol. Int. J.*, vol. 56, p. 101785, Aug. 2024, doi: 10.1016/j.jestch.2024.101785.

[3] S. Akhbar, N. S. N. Nik Omar, A. N. Mohd Yusof, S. Mohd Alauddin, and N. Kamarrudin, 'Preliminary study of melt flow index of recycled Polyethylene Terephthalate/Empty fruit bunch (rPET/EFB) composite as a potential biodegradable 3D printing filament', *Mater. Today Proc.*, vol. 87, pp. 366–369, Jan. 2023, doi: 10.1016/j.matpr.2023.03.625.

[4] A. Al Rashid and M. Koç, '3D-Printed recycled polyethylene terephthalate (PET) sandwich structures – Influence of infill design and density on tensile, dynamic mechanical, and creep response', *Int. J. Lightweight Mater. Manuf.*, vol. 8, no. 4, pp. 442–452, Jul. 2025, doi: 10.1016/j.ijlmm.2025.03.001.

[5] M. K. J. E. Exconde, J. A. A. Co, J. Z. Manapat, and E. R. Magdaluyo, 'Materials Selection of 3D Printing Filament and Utilization of Recycled Polyethylene Terephthalate (PET) in a Redesigned Breadboard', *Procedia CIRP*, vol. 84, pp. 28–32, Jan. 2019, doi: 10.1016/j.procir.2019.04.337.

[6] G. Kónya, L. Tóth, P. Gerse, F. Palásti, P. Hansághy, and F. Ronkay, 'Cutting tests and performance evaluation of recycled PET in fused filament fabrication', *Mater. Today Sustain.*, vol. 31, p. 101126, Sep. 2025, doi: 10.1016/j.mtsust.2025.101126.

[7] M. Nikam, P. Pawar, A. Patil, A. Patil, K. Mokal, and S. Jadhav, 'Sustainable fabrication of 3D printing filament from recycled PET plastic', *Mater. Today Proc.*, vol. 103, pp. 115–125, Jan. 2024, doi: 10.1016/j.matpr.2023.08.205.

[8] J. Mesicek *et al.*, 'Effect of part orientation and thickness on radiation shielding in FDM 3D printing of PET-G composite with tungsten', *J. Mater. Res. Technol.*, vol. 38, pp. 2886–2891, Sep. 2025, doi: 10.1016/j.jmrt.2025.08.080.

[9] L. Toth, E. Slezák, K. Bocz, and F. Ronkay, 'Progress in 3D printing of recycled PET', *Mater. Today Sustain.*, vol. 26, p. 100757, Jun. 2024, doi: 10.1016/j.mtsust.2024.100757.

[10] C. O'Driscoll, O. Owodunni, and U. Asghar, 'Optimization of 3D printer settings for recycled PET filament using analysis of variance (ANOVA)', *Heliyon*, vol. 10, no. 5, p. e26777, Mar. 2024, doi: 10.1016/j.heliyon.2024.e26777.

[11] A. Elik, 'Response surface methodology based on central composite design for optimizing temperature-controlled ionic liquid-based microextraction for the determination of histamine residual in canned fish products', *J. Food Compos. Anal.*, vol. 98, p. 103807, May 2021, doi: 10.1016/j.jfca.2021.103807.

[12] D. Alwazeer *et al.*, 'A Novel Hydrogen-incorporated Carbon Dioxide Supercritical System for Extracting Phytochemicals from Grape Peels: Response Surface Methodology–Based

Modeling and Optimization', *Results Eng.*, vol. 29, p. 109142, Jan. 2026, doi: 10.1016/j.rineng.2026.109142.
[13] N. S. Piro, 'Predictive modeling and optimization of sustainable ultra-high-performance concrete with response surface methodology', *Prog. Eng. Sci.*, vol. 3, no. 1, p. 100201, Mar. 2026, doi: 10.1016/j.pes.2025.100201.
[14] L. Xie, F. Wang, Z. Dou, J. Liu, K. Luo, and Y. Li, 'Modeling and multi-objective optimization of picosecond laser machining of blind holes in 4H-SiC using response surface methodology', *Mater. Sci. Semicond. Process.*, vol. 206, p. 110419, May 2026, doi: 10.1016/j.mssp.2026.110419.
[15] O. Pektezel and S. N. Ozdemir, 'Performance optimization of a three-stage cascade refrigeration system using response surface methodology', *Appl. Therm. Eng.*, vol. 287, p. 129446, Feb. 2026, doi: 10.1016/j.applthermaleng.2025.129446.
[16] L. Alidokht, K. A. Chavarria, and M. Lanzarini-Lopes, 'Optimizing energy budget for UV driven biofilm prevention using response surface methodology', *Environ. Technol. Innov.*, vol. 41, p. 104742, Mar. 2026, doi: 10.1016/j.eti.2025.104742.
[17] J. Andraskar and A. Kapley, 'Optimizing food waste composting with consortium, jaggery, and biochar using response surface methodology', *Bioresour. Technol. Rep.*, vol. 33, p. 102541, Feb. 2026, doi: 10.1016/j.biteb.2025.102541.
[18] Y. Yang, P. Zhao, L. Yu, J. Jia, and D. Zhu, 'Optimization of Supercritical CO2 Extraction of Juglone from Waste Walnut Green Husk via Response Surface Methodology', *J. Supercrit. Fluids*, p. 106886, Jan. 2026, doi: 10.1016/j.supflu.2026.106886.
[19] A. Mani and J. Sarkar, '3D simulation-based multi-objective optimization of segmented thermoelectric coolers using response surface methodology', *Appl. Therm. Eng.*, vol. 287, p. 129447, Feb. 2026, doi: 10.1016/j.applthermaleng.2025.129447.
[20] R. H. Myers, D. C. Montgomery, and C. M. Anderson-Cook, *Response Surface Methodology: Process and Product Optimization Using Designed Experiments*. John Wiley & Sons, 2011.
[21] C.-C. Liao and T.-W. Chung, 'Optimization of process conditions using response surface methodology for the microwave-assisted transesterification of Jatropha oil with KOH impregnated CaO as catalyst', *Chem. Eng. Res. Des.*, vol. 91, no. 12, pp. 2457–2464, Dec. 2013, doi: 10.1016/j.cherd.2013.04.009.
[22] T. K. Trinh and L. S. Kang, 'Application of Response Surface Method as an Experimental Design to Optimize Coagulation Tests', *Environ. Eng. Res.*, vol. 15, no. 2, pp. 63–70, Jun. 2010.
[23] V. Aggarwal, S. S. Khangura, and R. K. Garg, 'Parametric modeling and optimization for wire electrical discharge machining of Inconel 718 using response surface methodology', *Int. J. Adv. Manuf. Technol.*, vol. 79, no. 1, pp. 31–47, Jul. 2015, doi: 10.1007/s00170-015-6797-8.
[24] J. Yuan *et al.*, 'Multiple responses optimization of ultrasonic-assisted extraction by response surface methodology (RSM) for rapid analysis of bioactive compounds in the flower head of *Chrysanthemum morifolium* Ramat.', *Ind. Crops Prod.*, vol. 74, pp. 192–199, Nov. 2015, doi: 10.1016/j.indcrop.2015.04.057.
[25] S. Ahmadi, A. Khormali, and F. Meerovich Khoutoriansky, 'Optimization of the demulsification of water-in-heavy crude oil emulsions using response surface methodology', *Fuel*, vol. 323, p. 124270, Sep. 2022, doi: 10.1016/j.fuel.2022.124270.
[26] N. El-Gendy, S. Deriase, and A. Hamdy, 'The Optimization of Biodiesel Production from Waste Frying Corn Oil Using Snails Shells as a Catalyst', *Energy Sources*, vol. 36, Feb. 2014, doi: 10.1080/15567036.2013.822440.

[27] P. Biniaz, M. Farsi, and M. R. Rahimpour, 'Demulsification of water in oil emulsion using ionic liquids: Statistical modeling and optimization', *Fuel*, vol. 184, pp. 325–333, Nov. 2016, doi: 10.1016/j.fuel.2016.06.093.

[28] G. Sulochana and s. K. Bhatti, 'Performance and emission characteristics of a twin cylinder diesel engine blended biodiesel with nano additives using response surface methodology', *Int. J. Mech. Prod. Eng. Res. Dev.*, vol. 8, pp. 635–646, 2018.

[29] H. Karazhiyan, S. M. A. Razavi, and G. O. Phillips, 'Extraction optimization of a hydrocolloid extract from cress seed (*Lepidium sativum*) using response surface methodology', *Food Hydrocoll.*, vol. 25, no. 5, pp. 915–920, Jul. 2011, doi: 10.1016/j.foodhyd.2010.08.022.